

A lattice model of ternary mixtures of lipids and cholesterol with tunable domain sizes

Tanmoy Sarkar¹ and Oded Farago^{1,*}

¹*Department of Biomedical Engineering, Ben Gurion University of the Negev, Be'er Sheva 84105, Israel*
(Dated: March 7, 2023)

Much of our understanding of the physical properties of raft domains in biological membranes, and some insight into the mechanisms underlying their formation stem from atomistic simulations of simple model systems, especially ternary mixtures consisting of saturated and unsaturated lipids, and cholesterol. To explore the properties of such systems at large spatial scales, we here present a simple ternary mixture lattice model, involving a small number of nearest neighbor interaction terms. Monte Carlo simulations of mixtures with different compositions show an excellent agreement with experimental and atomistic simulation observations across multiple scale, ranging from the local distributions of lipids to the phase diagram of the system. The simplicity of the model allows us to identify the roles played by the different interactions between components, and the interplay between them. Importantly, by changing the value of one of the model parameters, we can tune the size of the liquid-ordered domains, thereby to simulate both Type II mixtures exhibiting macroscopic phase separation and Type I mixtures with nanoscopic domains. The Type II mixture simulation results fit well to the experimentally-determined phase diagram of mixtures containing saturated DPPC/unsaturated DOPC/Chol. When the tunable parameter is changed, we obtain the Type I version of DPPC/DOPC/Chol, i.e., a mixture not showing thermodynamic phase transitions but one that may be fitted to the same phase diagram if local measures are used to distinguish between the different states. Our model results suggest that short range packing is likely to be a key regulator of the stability and size distribution of biological rafts.

INTRODUCTION

Biological membranes are complex mixtures of many types of lipids, proteins and cholesterol (Chol) [1]. Though the lateral organization of such membranes is far from being fully elucidated, evidences indicate that it is highly heterogeneous [2]. Specifically, biological membranes contain small (10-200 nm) and dynamic domains, known as rafts, that are enriched in saturated lipids, cholesterol (Chol) and often particular proteins [2–4]. Rafts are liquid-ordered (L_o) domain “floating” in a sea of liquid-disordered (L_d) lipids [5, 6]. The L_d and L_o phase are liquid crystalline ones, where the lipids diffuse in the membrane plane [7]. In the L_o phase, the hydrocarbon chains are ordered, fully extended and tightly packed, similarly to the gel (S_o) phase [8]. Because of the enormous complexity of biological membranes, much of our understanding of the biophysical behavior and properties of raft domains is based on investigations of simple model membranes with few components, especially ternary mixtures of saturated and unsaturated lipids and Chol [9–13]. Studies of many different ternary mixtures reveal a phase diagram with regions of coexisting phases in the composition space, including coexistence between L_o and L_d phases which is believed to have relevance to raft domains in biological membranes [13–16]. Depending on the identity of the lipids and temperature, the L_d and L_o regions in ternary mixtures may be arranged in one of two ways: In mixtures like DPPC/DOPC/Chol [17] or DSPC/DOPC/Chol [18], for instance, they are thermodynamically (macroscopically)

phase separated over a wide range of compositions. In contrast, no true phase separation is observed when the doubly-unsaturated DOPC in these ternary mixtures is replaced with POPC, which has only one unsaturated hydrophobic chain. Instead, the liquid-ordered regions form small domains that are surrounded by a liquid-disordered matrix. This arrangement is commonly referred to as *microscopic phase separation* - a term that we also adopt here, emphasizing that it does not describe coexistence of phases in the thermodynamic sense. Feigenson [13] termed mixtures exhibiting thermodynamic (macroscopic) and “microscopic” phase separation as Type II and Type I mixtures, respectively. Type II mixtures show visible domains in fluorescence microscopy which makes their identification easy. In contrast, Type I mixtures appear uniform, and the presence of liquid-ordered domains in these systems must be inferred by indirect spectroscopic methods.

Generally speaking, formation of small and transient domains may be associated with a vanishingly small line tension between the liquid phases. In Type II mixtures, this is expected in the one phase region of the phase diagram close to the critical demixing point [16]. In the two phase region, a comparatively higher line tension drives the macroscopically large segregation of the liquid-ordered phases. Additionally, there are also other mechanisms that may lead to the appearance of small domains, including in Type I mixtures not exhibiting macroscopic phase separation (see recent reviews in [14, 19]), e.g., two dimensional microemulsion domains stabilized by line active molecules (lineactant) like hybrid lipids [20, 21], or a coupling between the local lipid composition and bilayer [22–24] or monolayer [25] curvatures. All of these mechanisms may be relevant to the formation of raft do-

* ofarago@bgu.ac.il

mains in biological membranes that are compositionally more complex and typically larger than liquid-ordered domains in Type I mixtures [19].

Accessing the length and time scales relevant to lipid domains in complex membranes is computationally very challenging. Atomistic simulation is the putative method for characterizing the molecular organization in lipid membranes [26]. It provides a molecular scale picture which is not available experimentally. However, even for simple model membranes, all-atom large scale simulations are computationally too costly. Therefore, a coarse-grained (CG) description is employed to allow access to the larger scales. In the past 15 years, CG simulations involving the MARTINI force-field have become very popular in the membrane biophysics community [27]. In MARTINI simulations, several atoms are unified and represented by effective beads. One particular problem of MARTINI simulations which often leads to inconsistencies with atomistic simulations of similar system, is the chain entropy which is heavily involved in the phase transition but is not properly represented when using a smaller number of effective beads (see review in [26] for examples of discrepancies between atomistic and MARTINI simulations of lipid-Chol mixtures). Beyond CG MARTINI (and similar force fields) simulations of *specific* lipids, we have more (ultra) CG *generic* models designed for studying the general mechanisms and biophysical driving forces governing the thermodynamic behavior of lipid mixtures [28]. The highest degree of abstraction and computational efficiency is offered by lattice models [29–38]. Lattice models have been extensively used as a tool for studying phase transitions, and many predictions of these models have proven to be relevant to lipid mixtures [31, 39]. Recently, we presented a lattice model for a binary mixture of the saturated lipid DPPC and Chol, that correctly captures the thermodynamic behavior of the system across multiple scales [40]. On the macroscopic scales, the lattice simulations reproduced the well-established phase diagram of DPPC/Chol mixtures, including regions where liquid-ordered domains of size ~ 10 -100 nm are observed in a liquid-disordered matrix. On the molecular scales, the simulations reveal the existence of gel-like nano clusters of size ~ 1 -10 nm within the larger Chol-rich liquid-ordered domains. Similar sub-structures have been seen in atomistic simulations of this system [41].

Fig. 1(i) shows the phase diagram of DPPC (saturated)/DOPC (doubly unsaturated)/Chol ternary mixture at $T = 283$ K. This canonical model system for studying the formation of liquid-ordered domains [16, 17, 42, 43] has been identified as a Type II mixture. Depending on the mole fractions of the lipids and Chol, the mixture may be found in a single or coexisting phases. Other Type II mixtures also show similar phase diagrams, where the exact location of the phase separating lines depends on the identity of the lipids and the temperatures. Curiously, many Type I ternary mixtures also feature phase diagrams resembling Fig. 1 (i) [44, 45], where the

liquid phases are microscopically rather than macroscopically separated. The presence of small ordered domains in Type I mixtures is inferred from studies based on different experimental methods, e.g., NMR [16], small-angle neutron scattering [46], X-Ray diffraction [47], and fluorescence resonance energy transfer (FRET) [38]. These observations can be interpreted in one of two ways: (i) a coexistence between two phases with extremely small line tension, or (ii) a single phase with local heterogeneities. From a theoretical point of view, the difference between these two interpretations is marginal, but if the latter interpretation is adopted then the liquid-liquid coexistence region in the phase diagram does not really exist. This controversy provides some of the motivation for the development of the model, presented herein, of ternary mixtures with tunable domain sizes. In the following, we present a minimal lattice model for a Type II mixture that fits very well the DPPC/DOPC/Chol phase diagram. The model contains a very small number of parameters, one of which directly controls the line tension between the disordered and ordered lipids. We demonstrate that by tuning the value of this parameter, we can change the nature of the mixture from Type II to Type I, i.e., convert macroscopically separated liquid phases into a mixture with traces of inhomogeneity at the local scale.

In atomistic and CG simulations, the presence of liquid-ordered domains is often based on visual inspection of the lateral organization and chain conformations of the lipids and Chol. One particular problem in computer simulations is the fact that the liquid-ordered domains may themselves be heterogeneous and contain nanoscopic gel-like clusters. The presence of such Chol-free hexagonally-packed clusters of acyl chains in liquid-ordered regions that are rich in Chol have been observed in simulations [40, 41] of binary DPPC/Chol mixtures, as well as in simulations of ternary DPPC/DOPC/Chol mixtures [48]. This local heterogeneous distribution of “domains within domains” is also consistent with experimental scattering data [49]. Another problem of detailed computer simulations are finite size effects. A simulation study of a ternary DPPC/DIPPC/Chol mixture has pointed that the nature of the two phase region and domain sizes may be strongly influenced by the size of the simulated system [50]. This may explain result of recent atomistic simulations of DPPC/DOPC/Chol mixtures where phase coexistence between liquid crystalline L_d and L_o is studied in a system consisting of ~ 1000 lipids [51]. That study, however, identified the system as a Type I mixture with domains of characteristic size of the order of 10 nm, which is in disagreement with clear experimental evidences indicating that this mixture is of Type II [17] featuring macroscopic phase separation. This, again, reinforces the importance of developing a computationally simple lattice model that allows simulations at large spatial and temporal scales. The attractiveness of lattice simulations lies not only in their computational simplicity, but also in their minimal nature which puts the focus on the factors that are essential

for understanding the biophysics of lipid mixtures and the mechanisms governing their thermodynamic phase behavior.

The DPPC/DOPC/Chol lattice model presented below is an extension of our recent successful lattice model of binary DPPC/Chol mixtures [40]. As will be shown below, the model provides a multiscale picture of the ternary mixture over an unprecedented wide range of scales. At the macroscopic scales, the model yields very nice agreement with the experimentally-derived phase diagram of this mixture, featuring all single and coexisting phases. At the microscopic scales, the model unravels the inhomogeneous nano scale distribution of lipids and Chol. Specifically, the model agrees with atomistic simulations showing that the liquid-ordered domains contain small gel cores of highly aligned DPPC chains [48]. The simplicity of the model helps identifying that the origin of these gel-like clusters can be attributed to the effective packing interactions of the saturated chains with each other and with the Chol. We further demonstrate that the strength of the packing interaction between ordered DPPC and DOPC chains controls the size of the domains. Thus, we can artificially eliminate the thermodynamic $L_d + L_o$ phase coexistence in DPPC/DOPC/Chol mixtures in favor of formation of smaller liquid-ordered domains. The resulting locally-inhomogeneous Type I mixture may be viewed as either a single phase or as thermally accessible configurations of a mixture of two coexisting liquid phases with a negligible line tension between them, and which quite surprisingly also fit the DPPC/DOPC/Chol phase diagram.

METHODS

The lattice model of ternary mixtures presented herein is based on the model of DPPC/Chol binary mixture

$$E = -\Omega_1 k_B T \sum_i \delta_{s_i,1} - \sum_{i,j} \epsilon_{22} \delta_{s_i,2} \delta_{s_j,2} - \sum_{i,j} \epsilon_{23} [\delta_{s_i,2} \delta_{s_j,3} + \delta_{s_i,3} \delta_{s_j,2}] - \sum_{i,j} \epsilon_{24} [\delta_{s_i,2} \delta_{s_j,4} + \delta_{s_i,4} \delta_{s_j,2}], \quad (1)$$

where the deltas are Kronecker deltas, and the summations are carried over all N_s lattice sites in the first term and over all nearest neighbor pair sites in the other terms. The first term in Eq. (1) accounts for the fact that the disordered state of the DPPC chains is entropically favored by a free energy, $-\Omega_1 k_B T$ (where k_B is Boltzmann constant and T is the temperature), over the ordered state. The other terms represent effective packing attraction between an ordered DPPC chain with another ordered DPPC chain (second term), Chol (third term), and DOPC chains (fourth term). For the model parameters in the first three terms in Eq. (1), we use the same values as in ref. [40]: $\Omega_1 = 3.9$, $\epsilon_{22} = 1.3\epsilon$

introduced in ref. [40]. Each chain is represented as a lattice point. Thus, the lipids with two acyl chains are represented as dimers while the Chol molecules occupy a single site. All Monte Carlo (MC) simulations are conducted on a triangular lattice of $N_s = 121 \times 140 = 16940$ (having an aspect ratio which is very close to unity) with periodic boundary conditions. The simulations are performed on a single planar lattice. This means that we do not explicitly introduce mechanisms speculated to be relevant for raft formation such as cross-monolayer interactions or curvature effects. A few lattice sites are left empty, thereby allowing the molecules to diffuse on the lattice which mimics the fluidity of the liquid membrane. The voids also allow the variations in the local density of the chains, which are expected in cases of coexistence between different phases. As in ref. [40], saturated DPPC chains may be in one of two states: ordered and disordered. Here, we introduce a second type of lipid with two unsaturated chains, say DOPC. These are always found in the disordered state because the system is simulated at temperatures higher than the low melting temperature of the DOPC. Thus, each lattice site obtains one of five possible states depending on the occupant: (i) a small area void ($s = 0$), (ii) a disordered ($s = 1$) or (iii) an ordered ($s = 2$) DPPC chain, (iv) a Chol ($s = 3$), (v) a DOPC chain ($s = 4$). In the lattice model, the detailed molecular picture of the forces between adjacent molecules is simplified and represented by nearest-neighbor interactions with effective parameters. The model Hamiltonian reads

and $\epsilon_{23} = 0.72\epsilon$, where the energy unit ϵ is such that the melting temperature of a pure DPPC membrane is $T_m = 314\text{K} = 0.9\epsilon/k_B$ [40, 52]. The values of the model parameters agree to order of magnitude with experimental data for the enthalpy change at the melting transition of DPPC vesicles.⁴ The fourth term account for the affinity between ordered DPPC and disordered DOPC chains,

⁴ The melting transition reflects a competition between the disordered and ordered states of the DPPC chains. The former is favored because of the entropy of the chains while the latter packs more efficiently with the surrounding chains. One should not expect ϵ_{22} to be in perfect agreement with the melting enthalpy

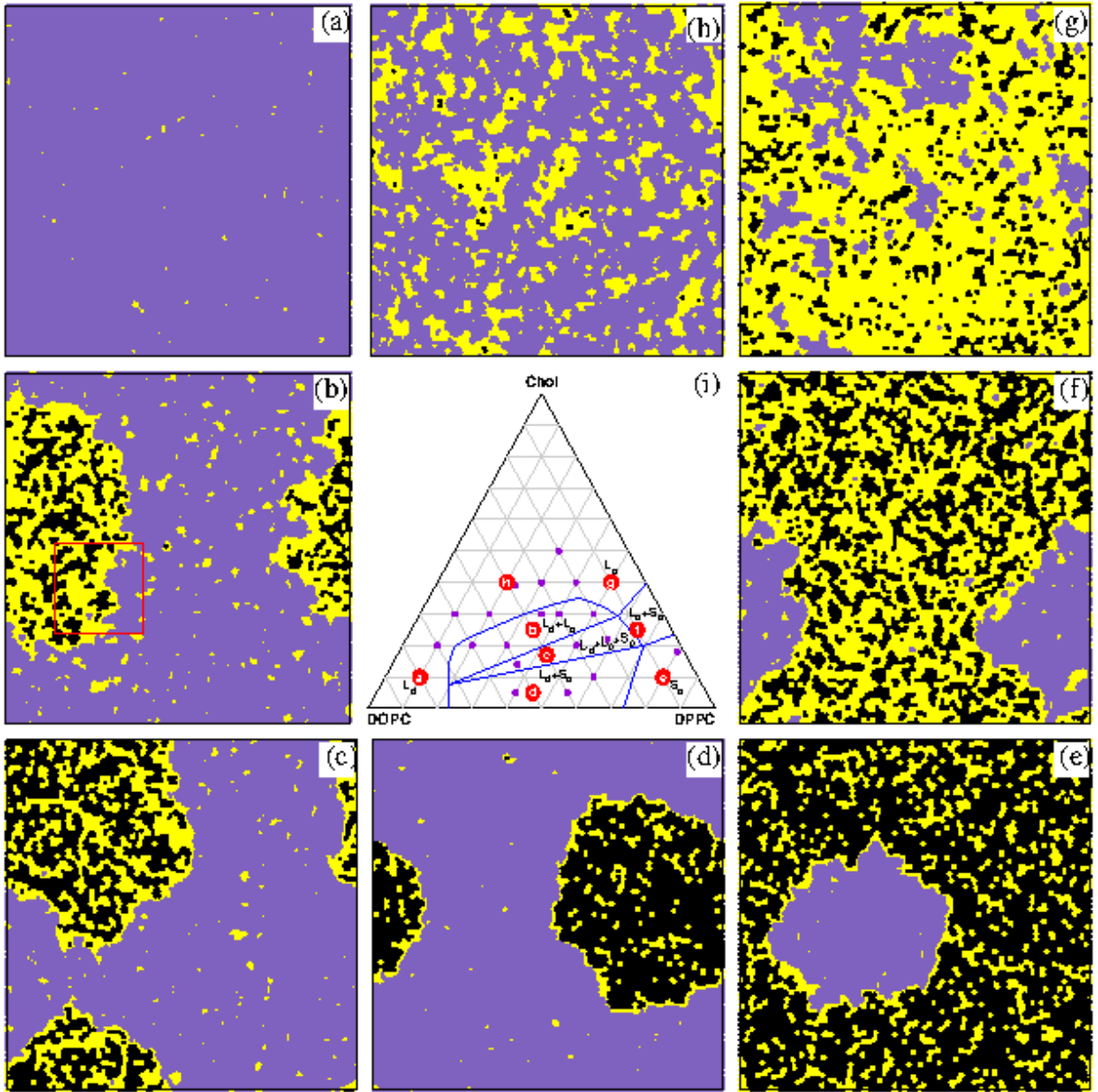


FIG. 1. Phase diagram and snapshots of the lateral organization of DPPC/DOPC/Chol mixtures at different compositions. The liquid-disordered (L_d), liquid-ordered (L_o), and gel (S_o) sites are colored in purple, yellow, and black, respectively. The snapshots are taken at temperature $T = 280$ K and for $\epsilon_{24} = 0$. Figure (a), (b), (c), (d), (e), (f), (g) and (h) show, respectively, snapshots from L_d , $L_d + L_o$, $L_d + L_o + S_o$, $L_d + S_o$, S_o , $L_o + S_o$, L_o and a single heterogeneous phase containing liquid-ordered domains in a liquid-disordered membrane. (i) Phase diagram of the ternary mixtures at $T = 283$ K. The blue phase separating lines are adapted from ref. [16]. The purple colored dots show the compositions of the simulated systems. The red dots with letters indicate the compositions of the snapshots.

thereby directly influencing their degree of mixing and controlling the line tension between the liquid-ordered and liquid-disordered regions. We consider two different values $\epsilon_{24} = 0.4\epsilon$ and $\epsilon_{24} = 0$. The latter result in a Type II mixture that fits nicely to the DPPC/DOPC/Chol phase diagram, while the former yields a Type I mixture with small liquid-ordered domains that arguably may be fitted to the very same phase diagram. Note that although we could include interaction terms between other components (and, thus, refine the results presented below), we prefer not to introduce such interactions in order to keep the model minimal and highlight only the essential biophysical driving forces.

The MC simulations employ the following move types: (i) Displacements and rotations of randomly chosen lipids and Chol molecules. Such moves are possible if the neighbor site is either empty or occupied by a Chol monomer, in which case the Chol swaps places with the displaced lipid chain, and (ii) a change in the state of a DPPC chain (ordered to disordered and vice versa). Simulations are conducted at temperatures of 280K or 310K, at which the area per DOPC lipid is $\simeq 0.67 \text{ nm}^2$ and $\simeq 0.73 \text{ nm}^2$, respectively [53]. At this temperature range, the areas per DPPC lipid and Chol are $\simeq 0.55 \text{ nm}^2$ and $\simeq 0.28 \text{ nm}^2$, respectively [41, 54]. We set the lattice spacing to $l = 0.56 \text{ nm}$, which means that the linear size of the simulation cell is $\simeq 70 \text{ nm}$. Depending on the composition of the simulated system, we set the number of voids such that the average density of the system matches the weighted average density of the constituting molecules. Systems are equilibrated for 10^{10} MC trail moves (95% of which are displacements and rotations and 5% are state exchange) until the memory of the initial configuration (either a random or a highly ordered distribution of the molecules on the lattice) is lost and the energy of the system relaxes to its characteristic value. We then continue to sample the system for 10^{11} MC trial moves during which we measure quantities of interest.

In the next section we present snapshots (see Figs. 1, 3, 4, and 6) where the sites of the lattice are drawn with distinct colors, denoting their belonging to liquid-disordered, liquid-ordered, and gel regions of the system. The partition of the sites into different categories is based in the following simple algorithm: The sites may be in one of five states: void, disordered DPPC chain, ordered DPPC chain, Chol, and DOPC chain. Each site is assigned with a score representing the degree of order of the associated state. Explicitly, liquid-ordered domains are rich in ordered DPPC and Chol, which receive positive scores of $Sc_i = 2$ and $Sc_i = 1$, respectively. Conversely, the liquid-disordered regions are populated with DOPC and disordered DPPC chains, which get negative scores of $Sc_i = -1$, and $Sc_i = -0.5$, respectively. Voids have a zero score. The *grade* of a site is given by

$$G_i = Sc_i + \sum_{j=1}^6 Sc_j \quad (2)$$

where the sum runs over the six nearest neighbors of the site. Sites with non-negative (negative) grades, $G_i \geq 0$ ($G_i < 0$), are associated with the liquid-ordered (liquid-disordered) regions. The maximum grade of $G_i = 14$ is obtained for ordered DPPC chains surrounded by 6 other ordered DPPC chains. These sites are marked as gel. After dividing the sites to the liquid-disordered, liquid-ordered, and gel regions, we scan the lattice one extra time and switch a liquid-disordered site to liquid-ordered if: (i) it is occupied by an ordered DPPC chain, and (ii) it has at least one neighbor belonging to a liquid-ordered or gel regions. The final iteration is needed in order to include ordered chains located at the periphery of the liquid-ordered domains that are surrounded by many disordered chains and incorrectly classified as part of the liquid-disordered regions.

For a given composition of components, we have generated many configurations starting at different initial distributions. We simulated the mixtures until they relax into states representing equilibrium and verified that different initial conditions evolve into similar phases: For instance, the snapshot in Fig. 1(b) shows a macroscopically large liquid-ordered domain in a liquid-disordered membrane (where some small liquid-ordered domains are also floating). This snapshot can be unambiguously interpreted as an indication that the equilibrium state of the mixture is a macroscopic $L_d + L_o$ phase coexistence. All other independent MC runs with the same compositions also evolve into similar structures corresponding to macroscopically phase separation between the two liquid phases. Our goal in this study is not to plot the exact locations of the boundaries of the phase diagram. These are adopted from experiments [16], and we investigate whether the outcomes of the simulations are consistent with the experimental phase diagram. Indeed, a visual inspection of the equilibrated systems shows good consistency with the experimentally determined phase diagram. Our lattice simulations results also show reasonable agreement with atomistic simulations data for the compositions of the liquid-disordered and liquid-ordered regions (see Table I below).

RESULTS

Type II DPPC/DOPC/Chol mixtures

Setting $\epsilon_{24} = 0$ in Eq. (1) for the DOPC interactions while keeping the values of the other model parameters as in our previous work on DPPC/Chol binary mixture [40], yields a ternary DPPC/DOPC/Chol Type II mixture model that reproduces the anticipated phase diagram. Our simulations at $T = 280\text{K}$ are summarized in Fig. 1. Fig. 1(a)-(h) show representative equilibrated snapshots from simulations with different compositions, the location of which in the ternary phase diagram are marked in red in Fig. 1(i). The purple points in Fig. 1(i) indicate additional simulated compositions whose snap-

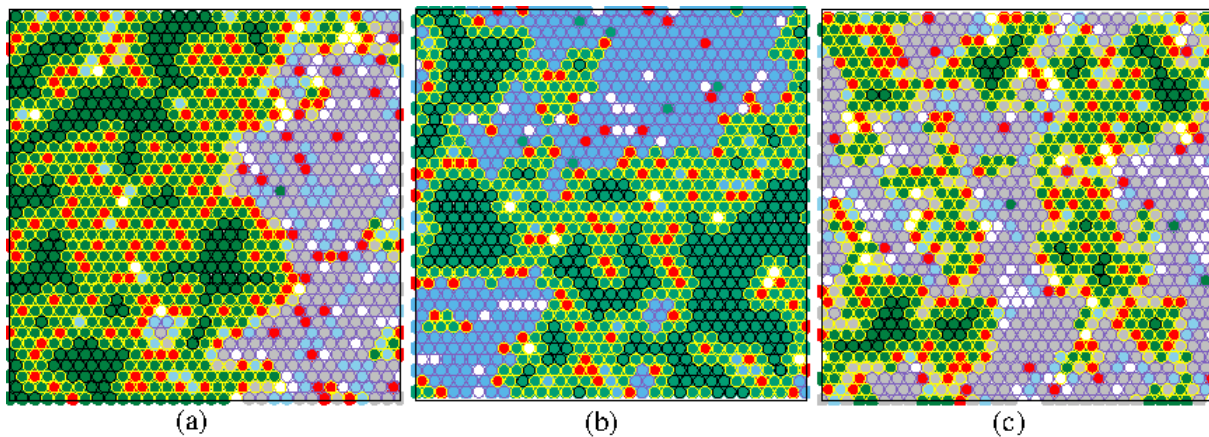


FIG. 2. Magnified views of small portions of (a) Type II ternary mixture, (b) binary mixture (adapted from ref. [40]), and (c) Type I ternary mixture. Ordered DPPC, disordered DPPC, DOPC, Chol, and empty sites are colored in green, light blue, grey, red, and white, respectively. Purple, yellow and black borders are assigned to the sites from liquid-disordered, liquid-ordered, and gel regions, respectively.

shots are not shown. In the snapshots, we color sites of the liquid-disordered, liquid-ordered, and gel regions with purple, yellow, and black, respectively. The blue lines in the phase diagram mark the experimentally-determined phase boundaries of DPPC/DOPC/Chol mixtures, as adapted from ref. [16]. We note that our aim herein is not to determine the phase lines but demonstrate that the model yield results that fit them. Indeed, we see in Fig. 1 that the snapshot configurations fit very well into the different regions in the phase diagram. DPPC/DOPC/Chol is a Type II mixture and, indeed, we observe in the two- and three-phase regions that the different phases are macroscopically segregated. At the microscopic scale, we notice that the different phases are locally inhomogeneous. This is best seen in fig 1(h) displaying a single inhomogeneous phase with liquid-ordered domains floating in a liquid-disordered sea. This near-critical arrangement, clearly differs from the $L_d + L_o$ coexistence appearing in snapshot (b).

Another example of a local inhomogeneity is seen in snapshot (g) of the L_o phase, where small gel clusters appear in the liquid-ordered region. Conversely, in the gel phase in snapshot (e), we see local liquid-ordered impurities. These inhomogeneities, which are also seen in snapshots (b) and (d) (where the L_o and gel phases coexist, respectively, with the L_d phase) represent local variations in the composition of the ordered regions. Recall that the sites marked by black color in the snapshots are the sites occupied by ordered DPPC chains with six ordered DPPC nearest neighbors. Since the gel phase in (e) also contains small amounts of Chol, not all of its sites, only most of them, can satisfy this criterion. Another notable observation in snapshot (e) of the gel phase is the segregation of a mesoscopic liquid-disordered domain containing mostly DOPC lipids. The presence of islands of disordered lipids within the ordered phases has also been observed experimentally [10]. The fluorescence mi-

croscopy micrographs appear as uniform L_o or S_o phases only when no DOPC is present. This experimental observation indicates that the unsaturated lipid has extremely low miscibility in the ordered phases. Despite the smallness of the liquid-ordered region, it must be admitted that it is more natural to interpret the appearance of a DOPC cluster in snapshot (e) as coexistence between gel and L_d phases, i.e., similarly to snapshot (d) but with different fractions of DOPC and DPPC. We note here that a single small liquid-disordered island was observed in simulations of mixtures with even lower amounts of DOPC (not shown), which raises the concern that our model parameters may not be accurately tuned and therefore result in excessively low miscibility of the DOPC lipids in the gel phase. In contrast to (e), in the L_o phase in snapshot (g), the segregation tendency of DOPC appears to be weaker and they form several smaller domains whose typical size falls below microscopic resolution. This looks like a mirror image of snapshot (h), and so the model adequately describes the continuous crossover between the L_d and L_o phases at moderate Chol concentrations.

Snapshot (f) exhibits intermediate properties of both the gel (e) and the L_o (g) phases, in terms of the relative fractions of gel and non-gel regions and the degree of segregation of the disordered part. One can therefore classify snapshot (f) as $L_o + S_o$ coexistence phase, although the separation is local rather than macroscopic (notice that the distribution of gel clusters inside the ordered region is locally inhomogeneous), and there seem to be a continuous crossover rather than a discontinuous transition between the L_o to gel phases. Likewise, snapshot (c) is recognized as a $L_d + L_o + S_o$ because of the intermediate nature between snapshots (b) and (d). We emphasize that the ability of our simulation snapshots to separate the disordered L_d phase from the ordered ones, while struggling to distinguish between the more similar ordered L_o and S_o phases is fully consistent with fluo-

rescence microscopy results where the same problem has been encountered [10]. Indeed, it has been noted that fluorescence microscopy alone is not well suited for studying the onset of the gel phase, and other experimental methods that are sensitive to smaller-scale lipid organization, e.g., NMR spectra, should be better suited for characterizing this putative three phase region. Our simulation results provide a picture of this local organization, suggesting that in the three phase region the L_d phase is macroscopically separated, while the L_o and S_o phases are segregated only at the local scales. In this context, it is important to remind that small gel clusters residing within the L_o phase have been also detected inside liquid-ordered domains in binary DPPC/Chol mixtures, suggesting that the thermodynamic origin of this observation is similar in both systems. This can be understood considering that the first three terms in Eq. (1) constitute the binary mixture Hamiltonian in ref. [40], and that we set to zero the coefficient in the fourth term accounting for the DOPC interactions. Thus, the picture inside the L_o phase remain quite similar, as demonstrated in Fig. 2 showing smaller portions of different simulated systems. Fig. 2(a) is a magnification of the region marked by a red square in snapshot (b) of Fig. 1. Depending on the state of the lattice site, it is marked by the following color: white ($s = 0$, void), light blue ($s = 1$, disordered DPPC chain), green ($s = 2$, ordered DPPC chain), red ($s = 3$, Chol), and grey ($s = 4$, DOPC chain). Additionally, the borders of the sites are marked with the same color coding as in the snapshots in Fig. 1 in order to indicate in which region (liquid-disordered - purple, liquid-ordered - yellow, and gel - black) they reside. Fig. 2(b) shows a magnified view from our previous simulations of DPPC/Chol mixtures [40], featuring similar local distributions of gel nano domains inside the liquid-ordered region. Fig. 2(c) is taken from our simulations of Type I ternary mixtures, to be presented in the following section [see red box in Fig. 4(b) below]. In Type I mixtures, the domains are smaller but, nevertheless, exhibit, similar local heterogeneities. The thermodynamic origin of these arrangements is the strong packing attraction between the ordered DPPC which drives their clustering into small gel domains. Chol, which prefers the vicinity of ordered DPPC chains (and, therefore, induces ordering of DPPC) is expelled from these clusters because its attraction to them is weaker than their mutual attraction. It accumulates in the liquid-ordered region, where it acts as a sort of a lineactant between the gel and the liquid-disordered region of the system.

The location of a second order critical point on the binodal curve separating the one phase and the two-phase $L_d + L_o$ regions is roughly near the intersection of binodal curve with the line corresponding to DOPC mole fraction, $\phi_{\text{DOPC}} = 0.4$ [along which points (h) and (b) reside] [16, 17, 42, 43]. The incomplete segregation of the system in (h) into small liquid-ordered domains and a liquid-disordered matrix is viewed as a precursor to the phase transition. According to this picture, the density

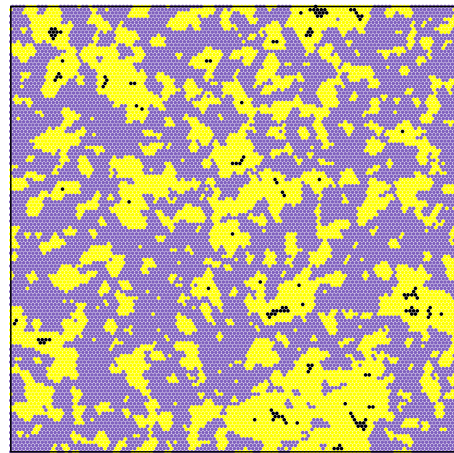


FIG. 3. A snapshot from the Type II mixture simulations at DPPC/DOPC/Chol mole fraction composition of 0.23:0.38:0.39 and $T = 280\text{K}$. Color coding is as in the snapshots in Fig. 1.

fluctuations in the one phase region are expected to intensify in the proximity of the critical point, leading to a broader distribution of domain sizes and the emergence of a percolation liquid-ordered cluster. Evidences supporting this scenario may be found in Fig. 3 showing a typical configuration DPPC/DOPC/Chol at mole fraction composition of 0.23:0.38:0.39. The distribution of liquid-ordered domain sizes is indeed broader here compared to Fig. 1(h) which, presumably, is located further from the critical point. Moreover, one can notice that the liquid-ordered domains in Fig. 3 almost percolate across the lattice.

To conclude this section, the simulation snapshots agree nicely with the experimental phase diagram regarding to one phase (L_d , L_o) and two-phase $L_d + L_o$ regions, including the estimated location of the second order critical point. As for the S_o gel phase, the miscibility of DOPC in this phase may be underestimated by the model which causes them, in the simulations, to phase separate and form small L_d domains that might be below macroscopic resolution. An interesting conclusion drawn from our simulations is the fact that the two ordered phases (L_o , S_o) exhibit local but not macroscopic separation. This observation is also consistent with experimental data, where $L_o + S_o$ coexistence has been inferred from spectroscopic methods that are sensitive to local details. In the following section dealing with Type I mixtures, we expand on the connection between scattering data and the detection of locally-separated phases in ternary mixtures.

Type I version of DPPC/DOPC/Chol mixtures

In the previous section we saw that in Type II mixtures, like DPPC/DOPC/Chol, small liquid-ordered domains are expected in the one phase region, i.e., above

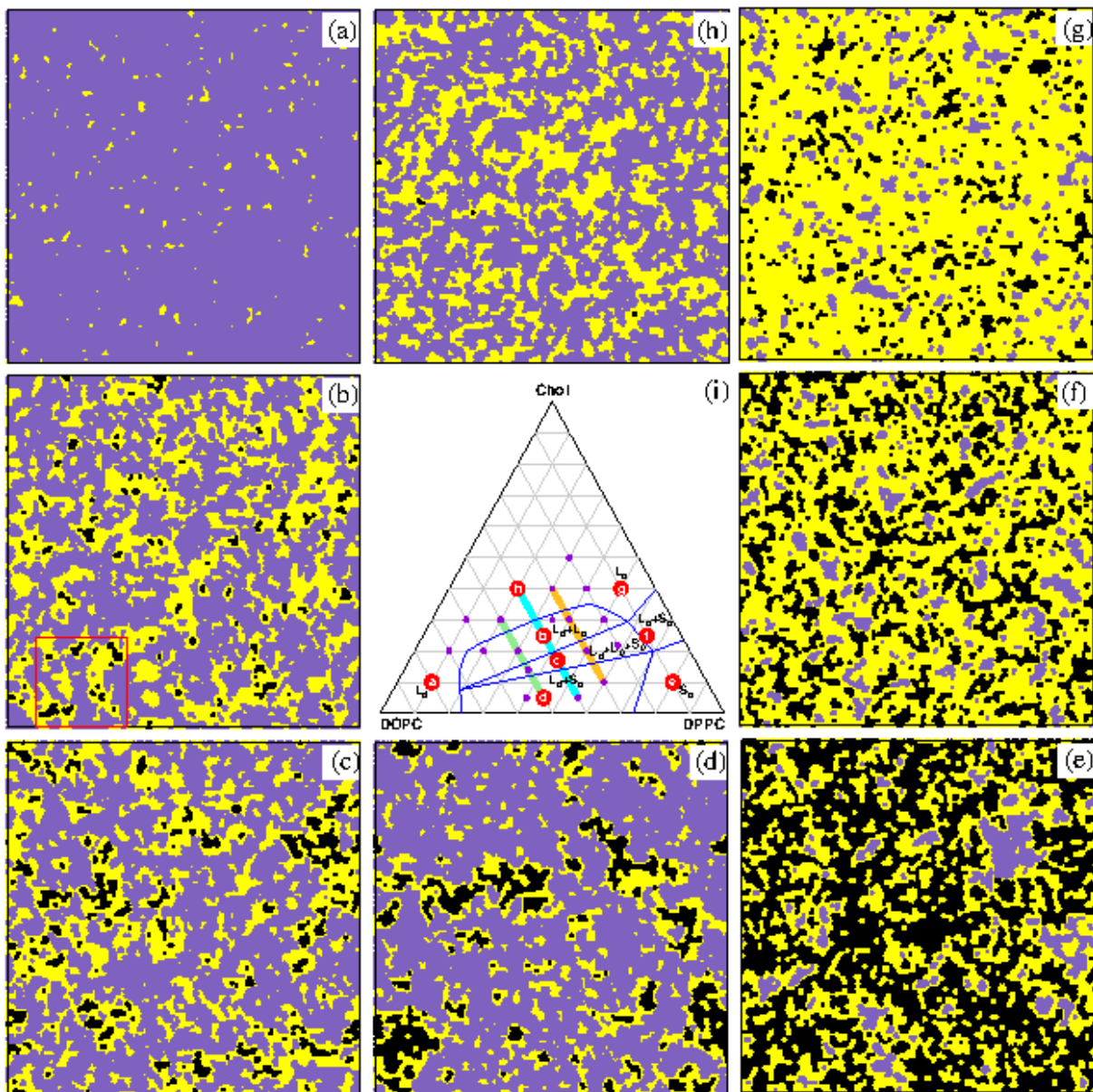


FIG. 4. Same as Fig. 1 but for $\epsilon_{24} = 0.4\epsilon$.

the binodal line but not too far from the critical point. But what about Type I mixtures that do not exhibit a true thermodynamic coexistence? In this section we demonstrate that such mixtures may still feature small liquid-ordered domains that float in the sea of a liquid-disordered membrane. Explicitly, we consider the same system as in the previous section and only change the value of the model parameter ϵ_{24} from 0 to 0.4, thereby allowing better mixing of the ordered DPPC and disordered DOPC chains. As we will now see, for this value of ϵ_{24} , the mixture may arguably be regarded as a Type I version of the Type II DPPC/DOPC/Chol mixture studied in the previous section: It lacks thermodynamic phase transition on the one hand, but fits the DPPC/DOPC/Chol phase diagram *if local measures are*

used to distinguish between the one phase and two phase regions.

Fig. 4 summarizes our simulation results at $T = 280\text{K}$ for $\epsilon_{24} = 0.4\epsilon$. The color coding used here is similar to the one in Fig. 1, and the phase diagram in (i) is identical to Fig. 1(i), i.e., drawn with the blue phase boundaries taken from [16]. One clearly sees that the change in the value of ϵ_{24} eliminates any signature of macroscopic phase separation, leaving only evidences of local phase separation, e.g., in snapshots (h), (b), (c), and (d). These snapshots indicate that the mixture is now of Type I. The question to be addressed now is whether the simulation snapshots in Figs. 4(a-h) still fit to the phase diagram in Fig. 4(i), which is the phase diagram of the Type II DPPC/DOPC/Chol ternary mixture. We first

note that snapshots (a), (g), and (e) are consistent with the expectations to observe single L_d , L_o , and S_o phases at the respective compositions. Identifying a two phase region when the system displays no macroscopic phase separation is, of course, harder. Snapshot (f), presumably showing coexisting L_o and S_o regions, exemplifies why the interpretation of the results is ambiguous. Recall that the gel regions are hexagonally packed arrangements of ordered DPPC chains. Therefore, we associate the gel phase in the snapshots with the lattice sites containing DPPC ordered chains with six nearest neighbors of the same kind. Both the liquid-ordered and gel phases appearing in (g) and (e), respectively, are highly populated with ordered DPPC chains. They differ in the fractions of chains obeying the six nearest neighbor criterion, which is high in (e) and low in (g). Looking at snapshot (f), one can interpret the observed distribution as a coexistence of regions of L_o and S_o phases, which are separated locally rather than macroscopically because of the smallness of the line tension between them. It is, however, impossible to rule out that the sequence of snapshots (e)-(f)-(g) simply shows a gradual decrease in the fraction of sites classified as gel. In this scenario, snapshot (f) is interpreted as a single phase which is locally inhomogeneous with regions that look more gel-like and regions resembling the liquid-ordered phase.

The main question pertains to the coexistence region of two liquid phases, $L_d + L_o$. As noted above, the justification for drawing the binodal curve in the phase diagram (i) is based on an ambiguous interpretation of scattering data. The detection of small domains below the resolution of optical microscopy is based on signals of local order in, e.g., FRET, NMR and electron spin resonance (ESR) spectroscopy [44, 55], but the results of such measurement do not resolve the question whether the ordered domains represent genuine phases or not. The problem is nicely exemplified by snapshots (h) and (b) which display visually similar distributions of liquid-disordered and liquid-ordered domains. These snapshots resemble the near-critical Type II mixture appearing in Fig. 3. The fact that we do not observe macroscopic phase coexistence in the present case does not necessarily rule out the possibility that snapshot (b) displays two-phase coexistence. This is because of the usual problem to distinguish between a single inhomogeneous phase and two-phase coexistence in the critical region where the mixture exhibits large thermal density fluctuations. Keep in mind that the snapshots in Fig. 4 show the classification of the lattice sites to different states (liquid-disordered/liquid-ordered/gel), but provide no real information about the local density fluctuations. Therefore, the boundaries between the ordered and disordered regions are probably fuzzier than appearing in the figures. With that said, we note that our state-classification algorithm works well and yields very good consistency with data from ref. [51] reporting on atomistic simulations of a Type I version of DPPC/DOPC/Chol mixtures. Table I lists the average compositions of the liquid-disordered and liquid-

TABLE I. Comparisons of lattice (this work) and atomistic (ref. [51]) simulations data for the average compositions of the liquid-disordered and liquid-ordered domains for mixtures with DPPC/DOPC/Chol mole fraction 0.35:0.35:0.30.

DPPC/DOPC/Chol composition			
Temperature (K)	model	liquid-ordered	liquid-disordered
280	Lattice	0.46:0.16:0.38	0.15:0.67:0.18
	Atomistic	0.53:0.13:0.34	0.16:0.60:0.24
310	Lattice	0.44:0.15:0.41	0.26:0.55:0.19
	Atomistic	0.48:0.14:0.38	0.20:0.60:0.20

ordered domains, measured for mixtures with overall DPPC/DOPC/Chol mole fraction of 0.35:0.35:0.30 (located in the $L_d + L_o$ region of the phase space). The agreement between the lattice and atomistic simulations is more than fair, even though that the domain classification algorithms used here and in ref. [51] are different. A visual inspection of different snapshots indicates that the domain sizes in both works are also similar. We note here that it is not clear why the atomistic simulations fail to exhibit the experimentally-observed macroscopic phase separation of DPPC/DOPC/Chol mixtures. It may be due to a problem with the force fields or an artifact of the small system size. We nevertheless use them as a benchmark for our simulations of the Type I version of DPPC/DOPC/Chol mixtures.

The problem lies not in the accuracy of the algorithm for classifying sites to liquid-disordered, liquid-ordered, and gel regions, but in its resolution. The algorithm, which is based on the inspection of the local vicinity of each lattice site, is too coarse to resolve the differences between configurations (h) and (b), and one must inspect more closely (i.e., define additional measures to quantify) the distribution of lipids at the nanometric small scales. In our model, we can gain such insight from the statistics of the ordered DPPC chains that are classified by the algorithm as either in the liquid-ordered or gel regions. (Ordered DPPC chains barely exist in the liquid-disordered region.) Explicitly, we check all these ordered DPPC chains and compute of the probability P_o of these chains to have $n_o = 0, 1, 2, 3, 4, 5, 6$ other ordered DPPC neighbors. Our analysis is summarized in Fig. 5 showing the statistics at four different points along the green, cyan, and orange lines appearing in Fig. 4(i). These lines, corresponding respectively to $\phi_{\text{DOPC}} = 0.5$ [statistics plotted in Fig. 5(a)], $\phi_{\text{DOPC}} = 0.4$ [Fig. 5(b)], and $\phi_{\text{DOPC}} = 0.3$ [Fig. 5(c)], cross four different parts of the phase space: the one phase region, two phase $L_d + L_o$, three phase $L_d + L_o + S_o$, and two phase $L_d + S_o$. The data in Fig. 5 suggests that the most distinguishing feature between configurations in the one phase and the $L_d + L_o$ two phase regions is the probability of having six ordered neighbors, which is quite negligible in the former and somewhat more substantial in the latter. This suggests that the presence of small gel clusters in the ordered domains is a defining property of the L_o phase. In the $L_d + S_o$ region, P_o is a monotonically increasing function

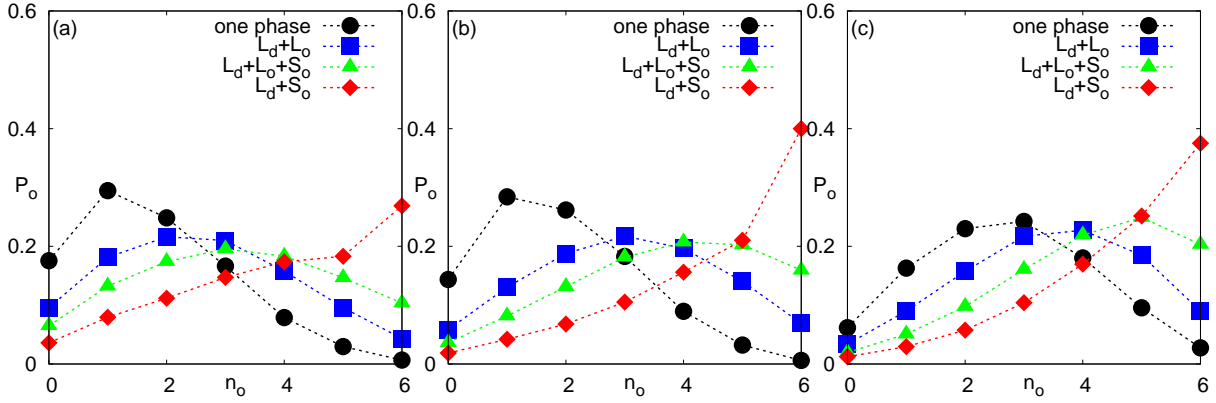


FIG. 5. The probability P_o of finding an ordered DPPC chain in the liquid-ordered and gel regions with n_o ordered DPPC nearest neighbors. Data in (a), (b), and (c) corresponding to simulations with $\phi_{\text{DOPC}} = 0.5, 0.4,$ and $0.3,$ respectively. For each $\phi_{\text{DOPC}},$ the statistics is calculated at four different compositions of systems belonging to the one phase (data plotted with black circles), two phase $L_d + L_o$ (blue squares), three phase $L_d + L_o + S_o$ (green triangles), and two phase $L_d + S_o$ (red diamond) parts of the phase space. Lines are guides to the eyes.

of $n_o.$ This is a characteristic feature of the gel phase. In the three phase region, the probability function exhibits features of both the $L_d + L_o$ and $L_d + S_o$ probabilities. As in the former, P_o is *not* monotonically increasing; but similarly to the latter, there is a significant probability to detect an ordered chain with $n_o = 6$ neighbors, indicating that the gel phase is also present.

To make an even closer connection with experimental data and provide more insight into the differences between regions of the phase diagram, we computed the spatial pair correlation function of local orderliness $g(r)$ and the associate Fourier transformation $|S(q)|.$ More precisely, the spatial correlation function is calculated from the grade function G_i used for the color coding of the snapshots in Figs. 1 and 4. Recall that the grade of a lattice point $G_i = G(x_i)$ is defined by Eq. (2) and assumes positive (negative) values for lattice points in the ordered (disordered) regions. To focus on the size of the ordered domains, we reset the grades of the disordered lattice points to zero, and calculate

$$g(r) \equiv \frac{\langle G(x_i)G(x_i + r) \rangle}{\langle G(x_i) \rangle^2} - 1, \quad (3)$$

where r is the pair distance between lattice points, and the averages are taken over all the lattice points x_i and over 100 independent snapshots of the system. The analysis is conducted at the same four compositions studied in Fig. 5(b) above, and summarized in Fig. 6(a). For all four compositions, which are located along the cyan line in different regions of the phase diagram Fig. 4(i), the function $g(r)$ is well fitted by a single exponential decaying function. The correlation length, which is inversely proportional to the slope of the lines in Fig. 6(a), serves as a measure for the characteristic linear dimension of the ordered domains. As expected from a visual inspection of snapshots, our results show that the size of the ordered domains grow as the composition of the mixture

is varied from the one phase region of the phase diagram to the $L_d + S_o$ region.

In reality, the pair correlation function of solids and dense liquids show oscillations at small distances because of the packing of the molecules. These oscillation are obviously absent in Fig. 6(a) because our data is taken from lattice configurations that provide no information at distances not corresponding to one of the lattice vectors. Therefore, Fig. 6(a) shows the envelope of the pair correlation function, from which we can extract information on the size of the domains. Insight into the internal domain structure and correlations can be gained from the model structure factor, $|S(q)|,$ defined by calculating the Fourier sum of the grade function $S(\vec{q}) = \sum_i G(x_i)e^{i\vec{q}\cdot\vec{x}_i},$ and then taking the angular average over all the orientations of the vector of size $\vec{q} = (q \cos(\theta), q \sin(\theta))^2:$

$$|S(q)| = \int_0^{2\pi} |S(\vec{q})| d\theta. \quad (4)$$

The model structure factor is plotted in Fig. 6(b) as a function of the wave-vector $q.$ For all four mixture compositions studied here, the central peak is located at the reciprocal lattice wave vector $q^* = 4\pi/\sqrt{3}$ (in units of inverse lattice spacing $l^{-1}).$ The magnitude of the peak increases when the composition of the mixture is varied from the one phase region to the $L_d + S_o$ region, reflecting the growth of the characteristic domain size along which the spatial correlation is maintained as seen in Fig. 6(a). Another trend observed in Fig. 6(b) is the increase in the amplitude and number of the satellite peaks around

² Because our simulations are conducted on a two-dimensional lattice we only take the average over the azimuthal angle. In X-ray scattering experiments of three-dimensional solutions, the average is over both the polar and azimuthal angles.

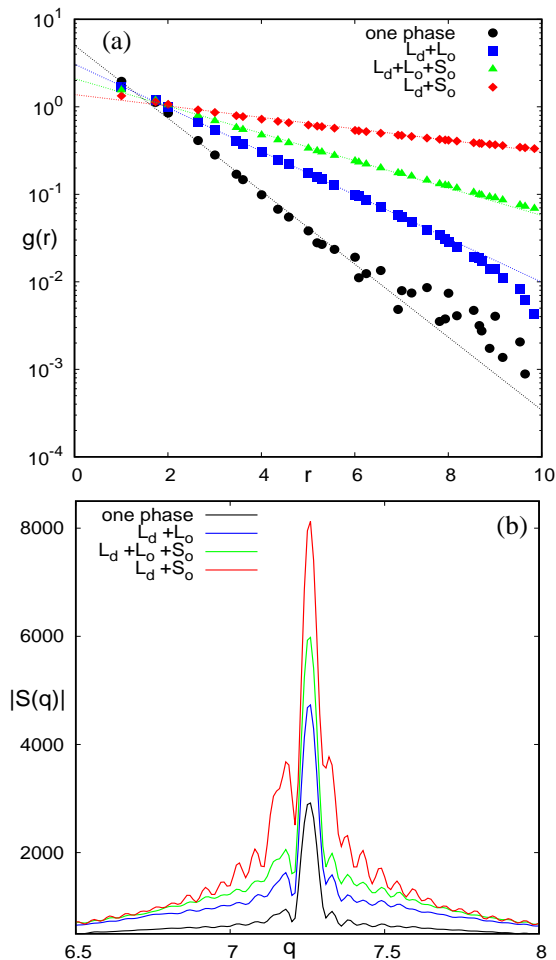


FIG. 6. (a) The pair correlation function defined in Eq. (3) as a function of the pair distance r (measured in units of the lattice spacing l), and (b) the associated model structure factor Eq. (4), as a function of the wave vector $q = |\vec{q}|$. The data corresponds to simulations of four mixtures with $\phi_{\text{DOPC}} = 0.4$ situated in the one phase (data plotted with black circles), two phase $L_d + L_o$ (blue squares), three phase $L_d + L_o + S_o$ (green triangles), and two phase $L_d + S_o$ (red diamond) regions of the phase diagram. Lines are guides to the eyes.

q^* . The satellite peaks serve as indicators for modulations in the orderliness of the domains. We can identify in Fig. 6(b) the differences between the phase space regions: In the one phase region we find a single weak satellite peak originating from the small domains floating in the mostly disordered mixture. In the $L_d + L_o$ region, the amplitude of this peak grows and a few more weak peaks appear. This is the contribution of the liquid ordered domains, especially the small gel-like regions inside them. When the gel clusters occupy a more substantial portion of the system, the number and amplitude of the satellite peaks increase significantly. We note here that we have verified (by visual inspection) that the appearance of many satellite peaks in the $L_d + S_o$ region does not arise because the system is frozen.

Type II mixture at physiological temperature

At $T = 310\text{K}$, most of the DPPC chains are found in the disordered state, which is understandable considering the proximity to their melting temperature $T_m = 314\text{K}$. At this temperature, a single L_d phase is expected throughout the entire phase diagram except, perhaps, for mixtures with a very high concentrations of DPPC [16]. Nevertheless, this phase may still contain small liquid-ordered domains, as demonstrated in Fig. 7, showing equilibrated configurations at compositions similar to points (b), (c), and (d) in Fig. 1 [denoted in Fig. 7 by (b2), (c2), (d2), respectively]. This is an important observation if one considers the ternary mixture model as a framework for understanding the formation of raft domains in biological membranes. As the snapshots in Fig. 7 demonstrate, our minimal model is capable of producing liquid-ordered domains of sizes $\lesssim 10$ nm even at the physiological temperature. These are local inhomogeneities with a characteristic correlational length which is half to one order of magnitude smaller than rafts in biological membrane, which is a well known limitation of experimental ternary mixtures [19]. This is why additional factors and mechanisms, e.g., curvature composition coupling [22–24, 56], as well as the presence of specific proteins and the cell cytoskeleton [57, 58], are believed to play a role in stabilizing larger domains. However, our results suggest that the same effect of increasing the domain sizes may be also accomplished by tuning differently the model parameters. After all, biological membranes are *not* ternary mixtures. They are composed of many lipid species with different melting temperatures and packing interactions, and our study suggests that even small changes in these parameters may affect dramatically the size distribution of the liquid-ordered domains.

DISCUSSION

We presented a simple lattice model for ternary mixtures of saturated and unsaturated lipids with Chol, involving only a minimal number of effective nearest-neighbor interactions between the constituting components. The model succeeds in explaining experimental and atomistic simulation observations across multiple scale, ranging from the local distributions of lipids to the macroscopic phase diagram. The model Hamiltonian is constructed by adding a single interaction term, between unsaturated (DOPC) and saturated lipids, to a previously presented model of a binary mixture of saturated lipids (DPPC) and Chol. The minimal nature of the model allows us to identify the influences of the different effective packing interactions and the underlying demixing mechanisms. The formation of the L_o phase is obviously related to the affinity of Chol to the saturated lipids. This phase is inhomogeneous and contains gel-like nano-clusters whose origin is the particularly strong attraction

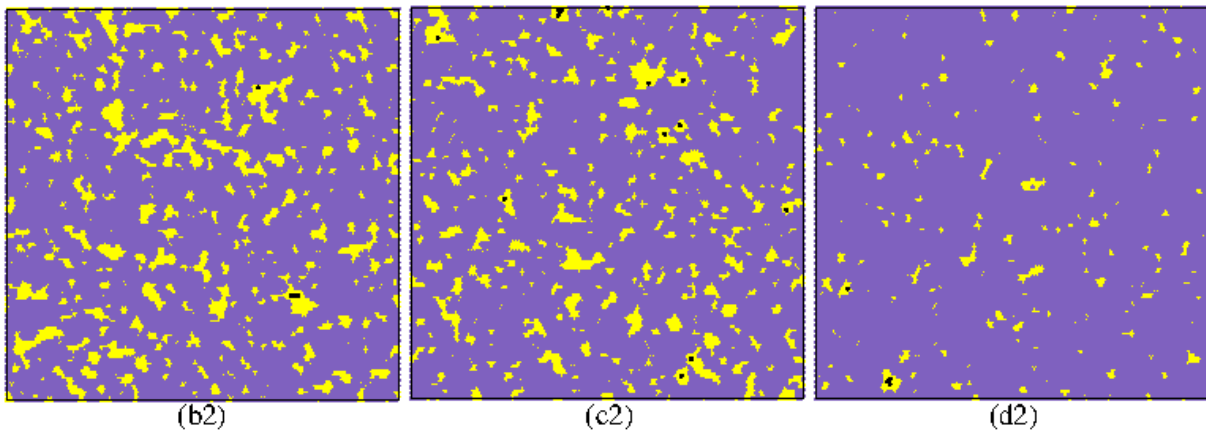


FIG. 7. Snapshots of equilibrated mixtures at temperature $T = 310$ K with $\epsilon_{24} = 0$. The compositions in (b2), (c2), and (d2) are the same as in (b), (c), and (d) in Fig. 1, respectively. Color coding is similar to Fig. 1.

of the saturated lipids to each other. The strength of the interaction between the unsaturated and saturated lipids, ϵ_{24} , controls the nature of phase transitions of the ternary mixture and the sizes of the liquid-ordered domains. For $\epsilon_{24} = 0$, the simulated mixture exhibits a macroscopic phase separation and fits nicely to the phase diagram of a Type II DPPC/DOPC/Chol mixture. In this case, liquid-ordered domains are observed in the one-phase region near the critical point of the $L_d + L_o$ coexistence binodal. For $\epsilon_{24} = 0.4$, we obtain the Type I version of a DPPC/DOPC/Chol mixture with nanoscopic domains. This system can be also fitted to the DPPC/DOPC/Chol phase diagram provided that local measures, such as the statistics of the ordered DPPC chains, are considered. In scattering experiments, nanometric features of this kind leave signatures in the scattering data, thus making the interpretation of configurations like in Fig. 4(b) ambiguous - either as coexistence of two liquid phases separated by a very small line tension or as a single phase with local inhomogeneities. Our aim here was not to decide which interpretation is correct, but to demonstrate that even if the phase transitions of the Type II DPPC/DOPC/Chol mixture are lost in the Type I version, local traces of phase coexistence still remain.

The motivation for studying lipid/Chol mixtures with a few components largely stems from the belief that they provide insight into the thermodynamic properties of cellular membranes. Because biological membranes are much complex physical systems, one should be cautious when coming to draw conclusions on their behavior from simpler model systems. On the one hand, the fact that biological membranes are mixtures of many differ-

ent types of lipids suggests that it may be possible to construct a suitable model with many interaction terms that not only shows formation of liquid-ordered domains, but also reproduces their size distributions (in contrast to ternary mixtures where the domains are usually smaller than biological rafts). Several recent theoretical studies of multi-component mixtures have indeed demonstrated that strong affinity of certain components to each other may lead to demixing phase transitions that are more robust with respect to variations in temperature and the intermolecular interactions than mixtures with a few components [59–61]. On the other hand, it would be probably wrong to ignore other mechanisms beyond short-range packing. This is particularly true for the inner cytoplasmic layer of cellular membranes that contains a low concentration of saturated lipids [62]. We can expect rafts to be influenced by the proximity to the cytoskeleton, the presence of proteins with affinities to certain lipids, and the curvature elasticity of the membrane (that depends on the local composition and induces coupling between the layers via the spontaneous curvature). Assessing the importance of these different mechanisms and understanding the interplay between them is going to remain an open question in the foreseeable future.

ACKNOWLEDGMENTS

This work was supported by the Israel Science Foundation (ISF), grant No. 991/17. TS thanks the Planning and Budgeting Committee of the Council for Higher Education (Israel) for supporting his post-doctoral fellowship.

[1] Alberts, B.; Johnson, A.; Lewis, J.; Raff, M.; Roberts, K.; Walter, P. *Molecular Biology of the Cell*, 4th ed.; Garland Science, New York, 2002.

[2] Levental, I.; Levental, K. R.; Heberle, F. A. Lipid rafts: Controversies resolved, mysteries remain. *Trends Cell Biol.* **2020**, *30*, 341.

- [3] Simons, K.; Ikonen, E. Functional rafts in cell membranes. *Nature* **1997**, *387*, 569.
- [4] Pike, L. Rafts defined: A report on the keystone symposium on lipid rafts and cell function. *J. Lipid Research* **2006**, *47*, 1597.
- [5] Van der Goot, F. G.; Harder, T. Raft membrane domains: From a liquid-ordered membrane phase to a site of pathogen attack. *Semin. Immunol.* **2001**, *13*, 89.
- [6] Kaiser, H.-J.; Lingwood, D.; Levental, I.; Sampaio, J. L.; Kalvodova, L.; Rajendran, L.; Simons, K. Order of lipid phases in model and plasma membranes. *Proc. Natl. Acad. Sci. U.S.A* **2009**, *106*, 16645.
- [7] Filippov, A.; Orädd, G.; Lindblom, G. Lipid lateral diffusion in ordered and disordered phases in raft mixtures. *Biophys. J.* **2004**, *86*, 891.
- [8] Holl, M. M. B. *Cell plasma membranes and phase transitions*, in: *Phase Transitions in Cell Biology*, Pollack, G. H.; Chin, W. C. (eds), Springer: Dordrecht, 2008.
- [9] Goñi, F. M.; Alonso, A.; Bagatolli, L. A.; Brown, R. E.; Marsh, D.; Prieto, M.; Thewalt, J. L. Phase diagrams of lipid mixtures relevant to the study of membrane rafts. *Biochim. Biophys. Acta Mol. Cell Biol. Lipids* **2008**, *1781*, 665.
- [10] Veatch, S. L.; Keller, S. L. Seeing spots: Complex phase behavior in simple membranes. *Biochim. Biophys. Acta, Mol. Cell Res.* **2005**, *1746*, 172.
- [11] Levental, I.; Veatch, S. L. The continuing mystery of lipid rafts. *J. Mol. Biol.* **2016**, *428*, 4749.
- [12] Chong, P. L.-G.; Zhu, W.; Venegas, B. On the lateral structure of model membranes containing cholesterol. *Biochim. Biophys. Acta Biomembr.* **2009**, *1788*, 2.
- [13] Feigenson, G. W. Phase diagrams and lipid domains in multicomponent lipid bilayer mixtures. *Biochim. Biophys. Acta Biomembr.* **2009**, *1788*, 47.
- [14] Komura, S.; Andelman, D. Physical aspects of heterogeneities in multi-component lipid membranes. *Adv. Colloid Interface Sci.* **2014**, *208*, 34.
- [15] Hirst, L. S.; Uppamoochikkal, P.; Lor C. Phase separation and critical phenomena in biomimetic ternary lipid mixtures. *Liq. Cryst.* **2011**, *38*, 1735.
- [16] Veatch, S. L.; Soubias, O.; Keller, S. L.; Gawrisch, K. Critical fluctuations in domain-forming lipid mixtures. *Proc. Natl. Acad. Sci. U.S.A* **2007**, *105*, 17650.
- [17] Veatch, S. L.; Keller, S. L. Separation of liquid phases in giant vesicles of ternary mixtures of phospholipids and cholesterol. *Biophys. J* **2003**, *85*, 3074.
- [18] Zhao, J.; Wu, J.; Heberle, F. A.; Mills, T. T.; Klawitter, P.; Haung G.; Costanza, G.; Feigenson, G. W. Phase Studies of Model Biomembranes: Complex Behavior of DSPC/DOPC/Cholesterol, *Biochim. Biophys. Acta. Biomembranes* **2007**, *1768*, 2764.
- [19] Schmid, F. Physical mechanisms of micro- and nanodomain formation in multicomponent lipid membranes. *Biochim. Biophys. Acta Biomembr.* **2017**, *1859*, 509.
- [20] Brewster, R.; Pincus, P. A.; Safran, S. A. Hybrid lipids as a biological surface-active component. *Biophys. J.* **2009**, *97*, 1087.
- [21] Palmieri, B.; Yamamoto, T.; Brewster, R. C.; Safran, S. A. Line active molecules promote inhomogeneous structures in membranes: theory, simulations and experiments. *Adv. Colloid Interface Sci.* **2014**, *208*, 58.
- [22] Leibler, S.; Andelman, D. Ordered and curved mesostructures in membranes and amphiphilic films. *J. Phys. France* **1987**, *48*, 2013.
- [23] Schick, M. Membrane heterogeneity: Manifestation of a curvature-induced microemulsion. *Phys. Rev. E* **2012**, *85*, 031902.
- [24] Sadeghi, S.; Müller, M.; Vink, R. L. C. Raft formation in lipid bilayers coupled to curvature. *Biophys. J.* **2014**, *107*, 1591.
- [25] Meinhardt, S.; Vink, R. L. C.; Schmid, F. Monolayer curvature stabilizes nanoscale raft domains in mixed lipid bilayers *Proc. Natl. Acad. Sci. U.S.A.* **2013**, *110*, 4476.
- [26] Enkavi, G.; Javanainen, M.; Kulig, W.; Róg, T.; Vattulainen, I. Multiscale simulations of biological membranes: The challenge to understand biological phenomena in a living substance. *Chem. Rev.* **2019**, *119*, 5607.
- [27] Marrink, S. J.; Risselada, H. J.; Yefimov, S.; Tieleman, D. P.; de Vries, A. H. The MARTINI force field: Coarse grained model for biomolecular simulations. *J. Phys. Chem. B* **2007**, *111*, 7812.
- [28] Meinhardt, S.; Schmid, F. Structure of lateral heterogeneities in a coarse-grained model for multicomponent membranes. *Soft Matter* **2019**, *15*, 1942.
- [29] Ipsen, J. H.; Karlström, G.; Mourtisen, O. G.; Wennerström, H.; Zuckermann, M. J. Phase equilibria in the phosphatidylcholine-cholesterol system. *Biochim. Biophys. Acta Biomembr.* **1987**, *905*, 162.
- [30] Caillé, A.; Pink, D.; De Verteuil, F.; Zuckermann, M. J. Theoretical models for quasi-two-dimensional mesomorphic monolayers and membrane bilayers. *Can. J. Phys.* **1980**, *58*, 581.
- [31] Almeida, P. F. A simple thermodynamic model of the liquid-ordered state and the interactions between phospholipids and cholesterol. *Biophys. J.* **2011**, *100*, 420.
- [32] De Joannis, J.; Coppock, P. S.; Yin, F.; Mori, M.; Zamorano, A.; Kindt, J. T. Atomistic simulation of cholesterol effects on miscibility of saturated and unsaturated phospholipids: Implications for liquid-ordered/liquid-disordered phase coexistence. *J. Am. Chem. Soc.* **2011**, *133*, 3625.
- [33] Heberle, F. A.; Feigenson, G. W. Phase separation in lipid membranes. *Cold Spring Harb. Perspect. Biol.* **2011**, *3*, a004630.
- [34] Dai, J.; Alwarawrah, M.; Ali, Md R.; Feigenson, G. W.; Huang, J. Simulation of the l_o - l_d phase boundary in DSPC/DOPC/Cholesterol ternary mixtures using pairwise interactions. *J. Phys. Chem. B* **2011**, *115*, 1662.
- [35] Reigada, R.; Buceta, J.; Gómez, J.; Sagués, F.; Lindenberg, K. Phase separation in three-component lipid membranes: From Monte Carlo simulations to Ginzburg-Landau equations. *J. Chem. Phys.* **2008**, *128*, 025102.
- [36] Banerjee, S.; Saha, J. A simulation study on multicomponent lipid bilayer. *Phys. A: Stat. Mech. Appl.* **2006**, *362*, 423.
- [37] Eckstein, J.; Berndt, N.; Holzhütter, H.-G. Computer simulations suggest a key role of membranous nanodomains in biliary lipid secretion. *PLoS Comput. Biol.* **2015**, *11*, e1004033.
- [38] Frazier, M. L.; Wright, J. R.; Pokorny A.; Almeida, P. F. F. Investigation of domain formation in sphingomyelin/cholesterol/POPC mixtures by fluorescence resonance energy transfer and Monte Carlo simulations. *Biophys. J.* **2007**, *92*, 2422.
- [39] Honerkamp-Smith, A. R.; Veatch, S. L.; Keller, S. L. An introduction to critical points for biophysicists; observations of compositional heterogeneity in lipid membranes. *Biochim. Biophys. Acta Biomembr.* **2009**, *1788*, 53.

- [40] Sarkar, T.; Farago, O. Minimal lattice model of lipid membranes with liquid-ordered domains. *Phys. Rev. Res.* **2021**, *3*, L042030.
- [41] Javanainen, M.; Martinez-Seara, H.; Vattulainen, I. Nanoscale membrane domain formation driven by cholesterol. *Sci. Rep.* **2017**, *7*, 1143.
- [42] Davis, J. H.; Clair, J. J.; Juhasz, J. Phase equilibria in DOPC/DPPC-d62/cholesterol mixtures. *Biophys. J.* **2009**, *96*, 521.
- [43] Uppamoochikkal, P.; Tristram-Nagle, S.; Nagle, J. F. Orientation of tie-lines in the phase diagram of DOPC/DPPC/cholesterol model biomembranes. *Langmuir* **2010**, *26*, 17363.
- [44] Heberle, F. A.; Wu, J.; LinGoh, S.; Petruzielo, R. S.; Feigenson, G. W. Comparison of three ternary lipid bilayer mixtures: FRET and ESR reveal nanodomains. *Biophys. J.* **2010**, *99*, 3309.
- [45] De Almeida, R. F. M.; Fedorov, A.; Prieto, M. Sphingomyelin/phosphatidylcholine/cholesterol phase diagram: boundaries and composition of lipid rafts. *Biophys. J.* **2003**, *85*, 2406.
- [46] Heberle, F. A.; Petruzielo, R. S.; Pan, J.; Drazba, P.; Kučerka, N.; Standaert, R. F.; Feigenson, G. W.; Katsaras, J. Bilayer thickness mismatch controls domain size in model membranes. *J. Am. Chem. Soc.* **2013**, *135*, 6853.
- [47] Clarke, J. A.; Heron, A. J.; Seddon, J. M.; Law, R. V. The diversity of the liquid ordered (Lo) phase of phosphatidylcholine/cholesterol membranes: a variable temperature multinuclear solid-state NMR and x-ray diffraction study. *Biophys. J.* **2006**, *90*, 2383.
- [48] Sodt, A. J.; Sandar, M. L.; Gawrisch, K.; Pastor, R. W.; Lyman, E. The molecular structure of the liquid-ordered phase of lipid bilayers. *J. Am. Chem. Soc.* **2014**, *136*, 725.
- [49] Armstrong, C. L.; Marquardt, D.; Dies, H.; Kučerka, N.; Yamani, Z.; Harroun, T. A.; Katsaras, J.; Shi, A.-C.; Rheinstädter, M. C. The observation of highly ordered domains in membranes with cholesterol. *PLoS ONE* **2013**, *8*, e66162.
- [50] Pantelopulos, G. A.; Nagai, T.; Bandara, A.; Panahi, A.; Straub, J. E. Critical size dependence of domain formation observed in coarse-grained simulations of bilayers composed of ternary lipid mixtures. *J. Chem. Phys.* **2017**, *147*, 095101.
- [51] Gu, R.; Baoukina, S.; Tieleman, D. P. Phase separation in atomistic simulations of model membranes. *J. Am. Chem. Soc.* **2020**, *142*, 2844.
- [52] Klump, H. H.; Gaber, B. P.; Peticolas, W. L.; Yager, P. Thermodynamic properties of mixtures of deuterated and undeuterated dipalmitoyl phosphatidylcholines (differential scanning calorimetry/lipid bilayers/membranes). *Thermochim. Acta* **1981**, *48*, 361.
- [53] Pan, J.; Tristram-Nagle, S.; Kučerka, N.; Nagle, J. F. Temperature dependence of structure, bending rigidity, and bilayer interactions of dioleoylphosphatidylcholine bilayers. *Biophys. J.* **2008**, *94*, 117.
- [54] Smondyrev, A. M.; Berkowitz, M. L. Structure of dipalmitoylphosphatidylcholine/cholesterol bilayer at low and high cholesterol concentrations: molecular dynamics simulation. *Biophys. J.* **1999**, *77*, 2075.
- [55] Yasuda, T.; Tsuchikawa H.; Murata M.; M. Nobuaki. Deuterium NMR of Raft Model Membranes Reveals Domain-Specific Order Profiles and Compositional Distribution. *Biophys. J.* **2015** *108*, 2502.
- [56] Allender, D.; Giang, H.; Schick, M. Model plasma membrane exhibits a microemulsion in both leaves providing a foundation for “rafts”. *Biophys. J.* **2020**, *118*, 1019.
- [57] Kusumi, A.; Nakada, C.; Ritchie, K.; Murase, K.; Suzuki, K.; Murakoshi, H.; Kasai, R. S.; Kondo, J.; Fujiwara, T. Paradigm shift of the plasma membrane concept from the two-dimensional continuum fluid to the partitioned fluid: High-speed single-molecule tracking of membrane molecules. *Annu. Rev. Biophys. Biomol. Struct.* **2005**, *34*, 351.
- [58] Fischer, T.; Vink, R. L. C. Domain formation in membranes with quenched protein obstacles: Lateral heterogeneity and the connection to universality classes. *J. Chem. Phys.* **2011**, *134*, 055106.
- [59] Girard, M.; Bereau, T. Finite-size transitions in complex membranes. *Biophys. J.* **2021**, *120*, 2436.
- [60] Carugno, G.; Neri, I.; Vivo, P. Instabilities of complex fluids with partially structured and partially random interactions. *Phys. Biol.* **2022**, *19*, 056001.
- [61] Jacobs, W. M.; Frenkel, D. Phase transitions in biological systems with many components. *Biophys. J.* **2017**, *112*, 683.
- [62] Lorent, J. H.; Levental, K. R.; Ganesan, L.; Rivera-Longsworth, G.; Sezgin, E.; Doktorova, M.; Lyman, E.; Levental, I. Plasma membranes are asymmetric in lipid unsaturation, packing and protein shape. *Nat. Chem. Biol.* **2020**, *16*, 644.